Study on the sensing characteristics of a local micro-structured long period fiber grating*

CAO Ye (曹晔), **PEI Yong-wei** (裴庸惟)**, **YANG Yin-fei** (杨寅飞), **and TONG Zheng-rong** (童峥嵘)
Key Laboratory of Film Electronics and Communication Devices, Tianjin University of Technology, Tianjin 300384, China

(Received 23 October 2013)

A simple and effective method employing a local micro-structured long period fiber grating (LMS-LPFG) for the simultaneous measurement of temperature and refractive index is proposed and investigated experimentally. The LMS-LPFG is formed by using the partial etching technique with hydrofluoric (HF) acid in a standard LPFG, in which there are discontinuities in the effective refractive index of cladding modes. Similar to the phase shift theory, a narrow passband and two stopbands are formed. The temperature and the surrounding refractive index (SRI) characteristics of the two stopbands and passband are studied. The temperature sensitivities of the two stopbands and passband are 0.05 nm/°C approximately. The SRI sensitivity of passband (-61.56 nm/RIU) is bigger than that of the two stopbands (-35.62 nm/RIU). Thus, with the sensitive matrix, we can simultaneously measure the changes of temperature and refractive index.

Document code: A **Article ID:** 1673-1905(2014)02-0129-4
DOI 10.1007/s11801-014-3208-6

Long period fiber grating (LPFG) has been widely used in optical fiber sensing and optical fiber communication[1]. Even so, LPFG still has some drawbacks, such as the discrimination of the cross-sensitivity between the surrounding refractive index (SRI) and temperature. Scholars did a lot of researches to solve this problem. In 2005, A. Iadicicco et al[2] made the first local micro-structured fiber Bragg grating (LMS-FBG) via partially etching the FBG, and thus a passband was produced in the stopband, similar to the phase shift grating (PSG). In 2012, Cao Ye et al[3] achieved a single grating to measure the temperature and surrounding refractive index (SRI) simultaneously by using the LMS-FBG. Yan Jinhua et al[4] demonstrated a new-type LPFG sensor by utilizing etching process on a dual-LPFG structure to simultaneously measure the SRI and temperature. Zhao Hongxia et al[5] proposed a semi-etched LPFG scheme for measuring the temperature and strain simultaneously. Similar to the LMS-FBG theory, L. R. Chen[6] proposed an approach for tuning the response of LPFG based on refractive index-shifting, and Kun-Wook Chung et al[7] designed a reconfigurable phase-shifted long period grating. In this paper, we present a new grating structure, which can simultaneously measure the liquid's SRI and temperature.

Fig.1 shows the schematic diagram of the LMS-LPFG. *BC* segment is etched by hydrofluoric (HF) acid. *AB* and *CD* segments are the original gratings. L_{TH} is the length of etched area, and D_{TH} is the diameter of etched cladding. In addition, according to the results of the experiment, it is low cost, tunable and with high resolution of refractive index.

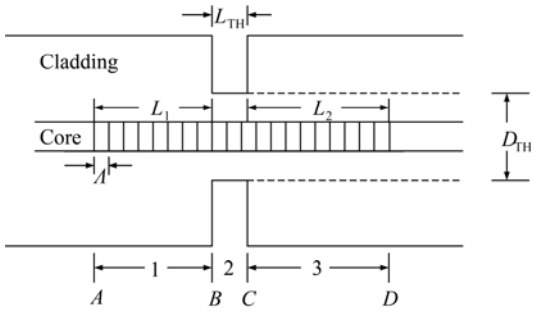

Fig.1 Schematic diagram of the structure of the LMS-LPFG

In a standard LPFG, according to the coupled mode theory, the phase matching between the core mode and the *m*th forward-propagating cladding mode is achieved at resonant wavelengths[8], given by

$$\lambda = (n_{\text{eff}}^{\text{co}} - n_{\text{eff}}^{\text{cl},m})\Lambda , \tag{1}$$

where $n_{\text{eff}}^{\text{co}}$ and $n_{\text{eff}}^{\text{cl},m}$ are the effective refractive indices of the core and the *m*th cladding mode, respectively, and Λ is the period of LPFG.

The coupled-mode equations of LPFG between the

* This work has been supported by the National Natural Science Foundation of China (No.61107052), and the Tianjin University's Science and Technology Development Fund Project (No.2012).
** E-mail: peiyongwei@126.com

core mode and the cladding modes can be written as

$$\frac{\mathrm{d}A_{\mathrm{co}}(z)}{\mathrm{d}z}=\kappa_{\text{co-cl}}A_{\mathrm{cl}}\mathrm{e}^{\mathrm{j}2\delta z}\mathrm{e}^{-\mathrm{j}\Phi}, \tag{2}$$

$$\frac{\mathrm{d}A_{\mathrm{cl}}(z)}{\mathrm{d}z}=-\kappa_{\text{co-cl}}A_{\mathrm{co}}\mathrm{e}^{-\mathrm{j}2\delta z}\mathrm{e}^{\mathrm{j}\Phi}, \tag{3}$$

where $A_{\mathrm{co}}(z)$ and $A_{\mathrm{cl}}(z)$ are the slowly varying amplitudes for the core mode and the cladding modes, respectively, δ is the phase mismatch, $\kappa_{\text{co-cl}}$ is the coupling coefficient, and Φ is the grating phase. When the effective refractive indices of the cladding modes are discontinuous, we use the piecewise uniform approach to express the solution to the coupled-mode equations[9]:

$$\begin{bmatrix}A_{\mathrm{co}}(z)\\A_{\mathrm{cl}}(z)\end{bmatrix}=F_N\cdot F_{N-1}\cdots\cdots F_2\cdot F_1\cdot\begin{bmatrix}A_{\mathrm{co}}(0)\\A_{\mathrm{cl}}(0)\end{bmatrix}, \tag{4}$$

with

$$F_i=\begin{bmatrix}\exp\left[\mathrm{i}\left(\bar{\beta}+\pi/\Lambda\right)\right] & 0\\ 0 & \exp\left[-\mathrm{i}\left(\bar{\beta}-\pi/\Lambda\right)\right]\end{bmatrix}\times$$
$$\begin{bmatrix}\cos(\gamma\Delta z)-\dfrac{\mathrm{i}\delta}{\gamma}\sin(\gamma\Delta z) & \dfrac{\mathrm{i}\cdot k_{\text{co-cl}}}{\gamma}\sin(\gamma\Delta z)\\ \dfrac{\mathrm{i}\cdot k_{\text{co-cl}}}{\gamma}\sin(\gamma\Delta z) & \cos(\gamma\Delta z)+\dfrac{\mathrm{i}\delta}{\gamma}\sin(\gamma\Delta z)\end{bmatrix}, \tag{5}$$

where $\gamma=\sqrt{k_{\text{co-cl}}{}^2+\delta^2}$, $\bar{\beta}=\frac{1}{2}\left(\beta_{\mathrm{co}}-\beta_{\mathrm{cl}}^i-\frac{2\pi}{\Lambda}\right)$, $\delta=\frac{1}{2}\times(\beta_{\mathrm{co}}-\beta_{\mathrm{cl}}^i)-(\pi/\Lambda)$, and β_{co} and β_{cl}^i are the ith section's propagation constants for the core mode and the cladding modes, respectively. For the LMS-LPFG, i=1 and 3 are for the non-etched grating sections, and i=2 is for the etched grating section.

In Fig.1, *BC* segment is etched by the HF acid, which induces the discontinuities of the cladding refractive index. According to the phase shift theory[10-13], a narrow allowed band will be formed, which is similar to PSG. However, unlike the conventional discrete phase shifted LPFG, the allowed band is tunable. The phase shift, which is related to the deviation of the propagation constant and the length of the defect, can be calculated by

$$\Phi=\frac{2\pi}{\lambda}\Delta n_{\text{eff\_cl}}L_{\mathrm{TH}}. \tag{6}$$

The cladding thickness influences the LPFG's sensitivity to surrounding material[14-16]. The LPFG can be more sensitive to SRI when the cladding's radius becomes smaller. The etched section is much more sensitive to SRI when the LPFG becomes thinner via partially etching.

For this simulation, the induced refractive index change in the core region is assumed as 1.8×10^{-5}, and the main resonant peak is selected at 1550 nm. The diameters of cladding and core are 125 μm and 8.3 μm, respectively, the grating length is 3.42 cm, and the grating pitch is 570 μm. The differential effective refractive index is 0.0275, L_{TH} is 1 cm and D_{TH} is 97.2 μm. The phase shift in the edge of etched region can be calculated as Φ= 0.98π.

Through the transmission matrix of MATLAB, the spectrum of the LMS-LPFG is obtained as shown in Fig.2.

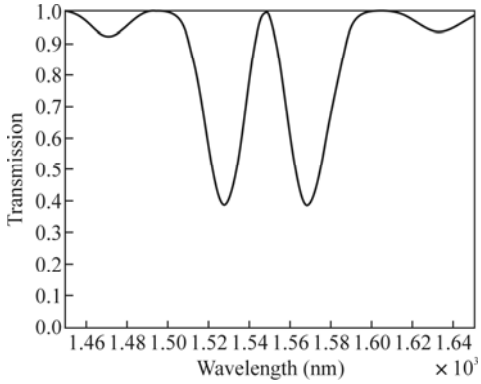

Fig.2 Simulation result for transmission spectrum of the LMS-LPFG

The sensitivity coefficients are different when the shifts of the stopband and allowed band are controlled by temperature and SRI. The responses of the LMS-LPFG to SRI and temperature can be expressed in matrix form as

$$\begin{bmatrix}\Delta\lambda_1\\ \Delta\lambda_2\end{bmatrix}=\begin{bmatrix}K_{T1} & K_{n1}\\ K_{T2} & K_{n2}\end{bmatrix}\begin{bmatrix}\Delta T\\ \Delta n\end{bmatrix}, \tag{7}$$

$$\begin{bmatrix}\Delta T\\ \Delta n\end{bmatrix}=\frac{1}{D}\begin{bmatrix}K_{n2} & -K_{n1}\\ -K_{T2} & K_{T1}\end{bmatrix}\begin{bmatrix}\Delta\lambda_1\\ \Delta\lambda_2\end{bmatrix}, \tag{8}$$

where $\Delta\lambda_1$ and $\Delta\lambda_2$ are the shifts of the stopband and allowed band, respectively, Δn is the change of SRI, ΔT is the change of temperature, K_{T1} and K_{n1} are the thermal coefficient and SRI coefficient of stop band, K_{T2} and K_{n2} are the thermal coefficient and SRI coefficient of allowed band, respectively, and $D=K_{T1}K_{n2}-K_{T2}K_{n1}$.

The LPFG used in our experiment is written by CO_2 laser. The diameters of core and cladding are 8.3 μm and 125 μm, respectively. The grating pitch is 570 μm, and the length of the grating is 3.42 cm. We made the grating in the middle of a plastic pipe whose length and radius are 1 cm and 0.2 cm, respectively. L_1 and L_2 are both 1.21 cm. We injected the HF acid into the plastic pipe, whose concentration is 20%. The LMS-LPFG was finally obtained after etching for about 40 min. The spectrum of the LMS-LPFG in experiment is shown in Fig.3.

We can see from Fig.3 that a narrow passband is formed in the middle of the resonant peak, and the peak of passband is 1543.60 nm, whereas the peaks of the double stopbands are 1539.72 nm and 1548.80 nm, respectively.

The schematic diagram of the experimental setup for

measuring temperature and refractive index simultaneously is shown in Fig.4. The left part is for the temperature measurement, and the right is for the SRI measurement.

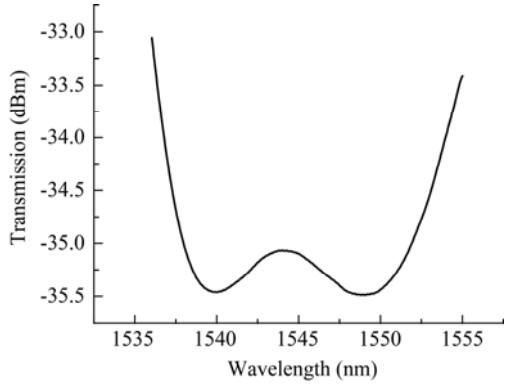

Fig.3 Experimental transmission spectrum of the LMS-LPFG

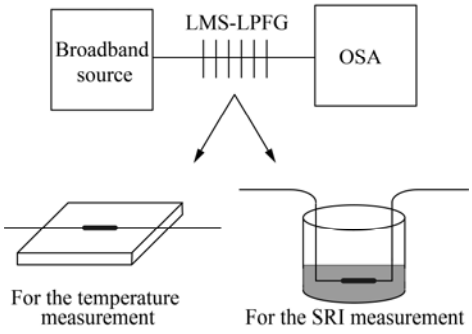

Fig.4 Experimental setup for measuring temperature and refractive index simultaneously

For the temperature measurement, the LMS-LPFG is placed into the thermostatic heater plate, and then the temperature is allowed to rise from 20 °C to 80 °C. The shifts of the peaks of double stopbands and passband are recorded every 5 °C. The fitted data is shown in Fig.5.

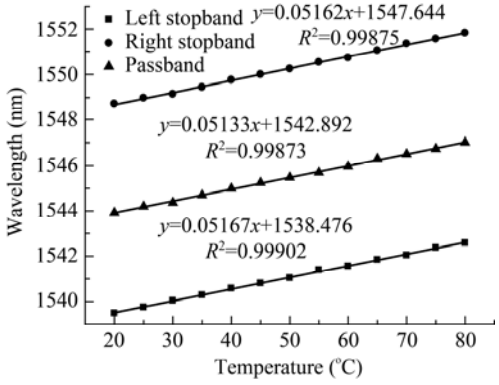

Fig.5 Temperature responses of the LMS-LPFG

From Fig.5 we can see that the three peaks all shift to the longer wavelength when the temperature is gradually increased. The shifts of the peaks of double stopbands are both 3.10 nm, and the shift of the passband peak is 3.08 nm. The temperature sensitivities of the three peaks are all 0.05 nm/°C approximately.

To get the SRI sensitivity of LMS-LPFG, we use a commercial Abbe refractometer. By increasing the concentration of NaCl, liquid samples with refractive indices varying from 1.33 to 1.38 are obtained. Then we place the LMS-LPFG into the NaCl solution, and observe the wavelength shifts in the optical spectrum analyzer (OSA). Fig.6 shows the SRI response of the LMS-LPFG. Obviously, a blue shift happens to all the three peaks when the refractive index is increased. However, the shift of passband's peak is 2.94 nm which is larger than those of the double stopbands' peaks, which are 1.70 nm and 1.71 nm, respectively. The SRI-sensitive coefficients can be calculated by the data fitting, which are 35.62 nm/RIU approximately for the two reflection peaks and 61.56 nm/RIU for the transmission peak.

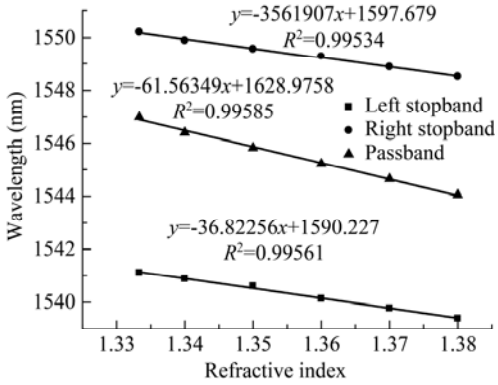

Fig.6 SRI responses of the LMS-LPFG

By substituting the coefficients into Eq.(8), we can get the relationship between the wavelength shifts and the changes of temperature and SRI in the following matrix as

$$\begin{bmatrix}\Delta T\\ \Delta n\end{bmatrix}=\frac{1}{-1.30}\begin{bmatrix}-61.56 & 35.62\\ -0.05 & 0.05\end{bmatrix}\begin{bmatrix}\Delta\lambda_1\\ \Delta\lambda_2\end{bmatrix}. \tag{9}$$

Therefore, the LMS-LPFG can deduce the changes of the liquid's refractive index and temperature simultaneously.

In conclusion, the influence of the partially etching technique in a standard LPFG is described and investigated. We fabricate a novel LMS-LPFG. There are discontinuities in the effective refractive index of the cladding modes which induce a narrow allowed band with the stopbands. With the thermostatic heater plate and NaCl solutions with different concentrations, we obtain the thermal coefficients and the refractive index coefficients of the three peaks. We can achieve the simultaneous measurement of SRI and temperature by the LMS-LPFG with the unique features. Due to the advantages of easy fabrication, high sensitivity and low cost, the proposed LMS-LPFG is convenient for practical use

and has potential applications in the chemical and biological sensing fields.

References

[1] SHI Sheng-hui, ZHOU Xiao-jun, ZHANG Zhi-yao and LIU Yong, Journal of Optoelectronics·Laser **23**, 1644 (2012). (in Chinese)

[2] A. Iadicicco, A. Cusano, S. Campopiano, Cutolo, Antonello and M. Giordano, IEEE Sensors Journal **5**, 1288 (2005).

[3] Ye Cao, Yinfei Yang, Xiufeng Yang and Zhengrong Tong, Chinese Optics Letters **10**, 030605 (2012).

[4] Jin-Hua Yan, A. P. Zhang, Li-Yang Shao and Jin-Fei Ding, IEEE Sensors Journal **7**, 1360 (2007).

[5] Zhao Hongxia, Cheng Peihong, Bao Jilong, Shen Hongkang, Li Lei and Du Huijian, Chinese Journal of Lasers **39**, 1205005 (2012). (in Chinese)

[6] L. R. Chen, Optics Communications **200**, 187 (2001).

[7] Kun-Wook Chung and Shizhuo Yin, Microwave and Optical Technology Letters **45**, 18 (2005).

[8] ZHANG Ling, MIAO Fei, SUI Qing-mei, Feng De-jun, LIU Han-ping and LIU Hui-lan, Journal of Optoelectronics·Laser **23**, 897 (2012). (in Chinese)

[9] Zheng-tian Gu, Xiao-yun Zhao and Jiang-tao Zhang, Optoelectronics Letters **5**, 244 (2009).

[10] Isa Navruz and Ahmet Altuncu, Journal of Lightwave Technology **26**, 2155 (2008).

[11] H. Ke, K. S. Chiang and J. H. Peng, IEEE Photonics Technology Letters **10**, 1596 (1998).

[12] Li Xiaolan, Zhang Weigang, Zhang Shanshan, Fan Hongjian and Yin Limei, Acta Optica Sinica **31**, 0606006 (2011). (in Chinese)

[13] LI Xiao-lan, ZHANG Wei-gang, SHANG Jia-bin and ZHANG Shan-shan, Journal of Optoelectronics·Laser **23**, 413 (2012). (in Chinese)

[14] Agostino Iadicicco, Stefania Campopiano, Michele Giordano and Andrea Cusano, Applied Optics **46**, 6945 (2007).

[15] Kin Seng Chiang, Yunqi Liu, Mei Nar Ng and Xiaoyi Dong, Electronics Letters **36**, 966 (2000).

[16] A. Martinez-Rios, D. Monzon-Hernandez and I. Torres-Gomez, Optics Communications **283**, 958 (2010).